Exploring Diverse Quadrupedal Gaits through Symmetry Breaking

Jiayu Ding, Zhenyu Gan

***Abstract*— Symmetry manifests itself in legged locomotion in a variety of ways: A legged system can maintain consistent gaits from any spatial starting point, exhibiting the same leg movements on either side of the torso in phase, and some even demonstrate forward and backward movements so similar they seem to reverse time. This work aims to generalize these phenomena and proposes formal definitions of symmetries in legged locomotion using terminology from group theory. In this research, we uncovered an intrinsic connection among a broad spectrum of quadrupedal gaits, which can be systematically identified via numerical continuations and distinguished by elements within a symmetry group. These gaits, within the hybrid dynamical system, are not merely isolated movements but part of a continuum, seamlessly transitioning from one to another at precise parameter bifurcation points. Altering specific symmetries at these junctures leads to the emergence of distinct gaits with unique footfall patterns, a phenomenon we've generalized through dimensional analysis in this study. Consequently, each gait manifests distinct preferred speed ranges and specific transition speeds.**

I. Introduction

The concept of *symmetries* has been widely used in the research of legged locomotion in order to reduce the complexity of the study, reveal fundamental differences among all gaits, and design locomotion controllers for legged robots. For example, Hildebrand (1965) used the phase delays among the leg pairs (front or hind) to categorize all the quadrupedal gaits [1]. If the phase delay in the gait is equal to half of the stride cycle, he called it a *symmetrical gait*; otherwise, an *asymmetrical gait*. He suggested that all the symmetrical gaits and asymmetrical gaits formed two distinct continua [2] and animals like horses can smoothly switch from one gait to another if they are closely related. Another type of symmetry was brought up by Marc Raibert (1986) from his early studies of running legged robots, in which he found when the robot was moving backward, it was almost the same as moving forward in a time-reversed fashion [3]. More recently, Razavi *et al.* (2017) introduced a new method to design stable periodic walking gaits for legged robots based on producing a type of odd-even symmetry in the system [4]. This approach can identify symmetries in the system dynamics and generate periodic walking without relying on any kind of numerical search. And the study of symmetries has been proven useful for data-driven analysis of robotic systems [5]. By recognizing and exploiting data symmetries through the use of invariant neural networks (NN), symmetry constraints can lead to better sample efficiency and reduce the number of trainable parameters. In this study, we try to leverage the existing studies of symmetries in legged locomotion [6] and group theory [4] and seek to understand the inherent relationships among the large number of asymmetrical gaits observed by Hildebrand [7].

Jiayu Ding and Zhenyu Gan are with the Mechanical and Aerospace Engineering, Syracuse University, Syracuse, NY 13244 {jding14, zgan02}@syr.edu . This work was supported by a startup fund from Syracuse University. It was accepted by IEEE RA-L in March 2024. For citation, please use DOI: 10.1109/LRA.2024.3384908.

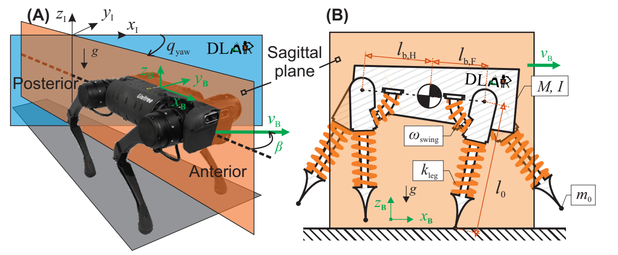

Fig. 1. (A) A1 quadrupedal robot from Unitree Robotics with bilateral symmetry and (B) a simplistic spring-mass model.

II. Methods

Symmetries of mechanical systems are natural examples of group actions, and they often provide a useful mechanism to reduce the complexity of the problem by reducing the number of variables. The motion of a legged system can be modeled as a hybrid system Σ that consists of a set of differential-algebraic equations $\mathcal{F}$ describing the continuous dynamics of the robot in each domain and a set of impact maps Δ that instantaneously reset the velocities. The global behavior of such systems has been explored in the literature, notably in [4], [8]. In this work, in order to focus on quadrupedal locomotion with diverse footfall patterns, we conduct a local symmetry analysis on the periodic solutions of such systems. A gait of a legged system is defined as:

Definition 1 (Gait): Suppose the equations of motion of a quadrupedal robot can be modeled as a continuous time ($t \in \mathbb{R}$) hybrid system $\Sigma(t)$ on phase space $\mathcal{X}$, where $\boldsymbol{x} \in \mathcal{X}, \boldsymbol{x}(t) := [\boldsymbol{q}(t)^\intercal, \dot{\boldsymbol{q}}(t)^\intercal]^\intercal$. It is also assumed that in each stride every leg is limited to a single strike and lift-off. The dynamics of $\Sigma(t)$ is given by an evolution operator $\boldsymbol{\varphi}_t(\mathcal{X} \rightarrow \mathcal{X}) : \boldsymbol{x}(\tau) \mapsto \boldsymbol{x}(\tau + t)$. We consider a *gait* of a legged robot as a periodic orbit $\mathcal{O} \subset \mathcal{X}$ *i.e.*, there exists a finite $T > 0$ such that $\mathcal{O} = \{\boldsymbol{x}(t) \mid \boldsymbol{S}\boldsymbol{x}(t) = \boldsymbol{S}\boldsymbol{\varphi}_T(\boldsymbol{x}(t)) = \boldsymbol{S}\boldsymbol{x}(t+T)\}$, where $\boldsymbol{S} = diag(0, 1, 1, 1...)$ is the selection matrix, which excludes the horizontal position q_x from the periodicity.

In this definition, we assume the evolution operator φ_t is unique in both forward time ($t > 0$) and backward time ($t < 0$). Given this assumption, we generalize the symmetries of gaits through group theory, defining a symmetry as a group action that transforms one gait into another:

Definition 2 (Symmetry): For any gait $\mathcal{O}$, the symmetries form a group G. A symmetry of G on the gait $\mathcal{O}$ is an assignment of a function $\mathcal{S}_g : \mathcal{O} \to \mathcal{O}$ to each element $g \in G$ in such a way that:

- If I is the identity element of the group G, then $\mathcal{S}_I$ is the identity map, *i.e.*, for every gait $\mathcal{O}$ we have $\mathcal{S}_I(\mathcal{O}) = \mathcal{O}$.
- For any $g, h \in G$, we have $\mathcal{S}_g \circ \mathcal{S}_h = \mathcal{S}_{gh}$, *i.e.*, for every gait $\mathcal{O}$, we have $\mathcal{S}_g\left(\mathcal{S}_h(\mathcal{O})\right) = \mathcal{S}_{gh}(\mathcal{O})$;
- For any $g \in G$, there exists the inverse of g such that $\mathcal{S}_g \circ \mathcal{S}_{g^{-1}} = \mathcal{S}_I$;

1) Temporal Symmetry: Since gaits are periodic, starting from any point on the orbit, all states will return to their original value after every T seconds. This gives us the first kind of discrete symmetry about time. The periodicity of the states also suggests the conservation of linear and angular moment in each direction over every T second.

Definition 3 (Temporal Symmetry): Suppose there are no energy losses related to the impact map Δ, there exists a finite $T > 0$ and specific timings $t = nT$ ($n \in \mathbb{Z}^+$), and the evolution operator $\boldsymbol{\varphi}_t$ forms a subgroup named temporal symmetry $\boldsymbol{\varphi}_{nT}$ such that $\boldsymbol{\varphi}_{t_1} \circ \boldsymbol{\varphi}_{t_2} = \boldsymbol{\varphi}_{t_1+t_2}$ for all $t_1, t_2 \in nT$ and $\boldsymbol{\varphi}_t^{-1} = \boldsymbol{\varphi}_{-t}$, in which $-t$ corresponds to reversing the motion and rewinding time for every gait. Specifically, assume a state vector on the orbit takes the form $\boldsymbol{x}(t) = [\boldsymbol{q}_T(t)^\intercal, \boldsymbol{q}_L(t)^\intercal, \dot{\boldsymbol{q}}(t)_T^\intercal, \dot{\boldsymbol{q}}(t)_L^\intercal]^\intercal \in \mathcal{O}$, the temporal symmetry is a function $\mathcal{S}_\varphi : \boldsymbol{x}(t) \to \boldsymbol{x}(t)$:

$$\begin{aligned}\mathcal{S}_\varphi : &[\boldsymbol{q}_T(t)^\intercal, \boldsymbol{q}_L(t)^\intercal, \dot{\boldsymbol{q}}_T(t)^\intercal, \dot{\boldsymbol{q}}_L(t)^\intercal]^\intercal, \\ &\mapsto \boldsymbol{\varphi}_{nT}\,[\boldsymbol{q}_T(t)^\intercal, \boldsymbol{q}_L(t)^\intercal, \dot{\boldsymbol{q}}_T(t)^\intercal, \dot{\boldsymbol{q}}_L(t)^\intercal]^\intercal\end{aligned} \tag{1}$$

Even though once a gait is identified, in theory, we can always rewind the time and find the inverse mapping of the evolution operator, in reality, this process is usually nonphysical and cannot be realized on the hardware. Under the presence of damping, friction, or collisions, the reverse mapping requires the legged system to reverse the energy flow and absorb energy from its environment. Additionally, when the projection Δ is non-invertible, the solutions of a hybrid system are often not unique in backward time. However, it has been commonly observed that both humans and quadrupedal animals utilize similar gaits when moving both forward and backward [3]. Also, as a theoretical study, this is still a very interesting phenomenon for many idealized energetically conservative models, such as SLIP models proposed in the previous section. Here we only consider a special instance when the energy in the system is reversible and the reset map is continuous *i.e.*, an identity map, then we have the following discrete symmetry:

Definition 4 (Time-Reversal Symmetry): The time reversal symmetry is an action of G_ψ on the gait $\mathcal{O}$ endowed with a function $\mathcal{S}_\psi$ that reverses the velocities:

$$\begin{aligned}\mathcal{S}_\psi : &[\boldsymbol{q}_T(t)^\intercal, \boldsymbol{q}_L(t)^\intercal, \dot{\boldsymbol{q}}_T(t)^\intercal, \dot{\boldsymbol{q}}_L(t)^\intercal]^\intercal, \\ &\mapsto \boldsymbol{\varphi}_{nT}\,[\boldsymbol{q}_T(t)^\intercal, \boldsymbol{q}_L(t)^\intercal, -\dot{\boldsymbol{q}}_T(t)^\intercal, -\dot{\boldsymbol{q}}_L(t)^\intercal]^\intercal\end{aligned} \tag{2}$$

This symmetry implies that when a robot faces forward while moving backward, it is identical to moving forward in a time-reversed fashion. This definition of symmetry has been discussed by Marc Raibert on his bipedal hopping robot and quadrupedal bounding robot [3]. The reverse motion also satisfies the same set of EoMs as the forward motion and one cannot decide whether the system is moving forward or backward just by looking at the motion pictures [9].

2) Spatial Symmetry: The environment of the system also has huge effects on the symmetries of gaits. As we modeled legged systems as FBMs in the Euclidean space, they are known for having symmetries to translations and rotations. If there is no gravity in the environment and the robot is floating in space, every transformation $SE(3)$ of the torso's state is a symmetry that preserves the mass and inertia of the bodies and the linear/angular momentum of the robot. As soon as the robot is subjected to gravity and constrained to move on a surface, it breaks the spatial symmetry of the system. Here, for simplicity, we only consider the ground (moving surface) to be flat and perpendicular to the gravitational field.

Definition 5 (Spatial Symmetry): Given the assumptions above, the 2 dimensional Euclidean isometries $SE(2)$ form a continuous symmetry subgroup $G_\xi \subset G$ of a gait $\mathcal{O}$. An action of G_ξ on the gait $\mathcal{O}$ is an assignment of a function $\mathcal{S}_\xi : \mathcal{O} \to \mathcal{O}$ to each element $\xi \in G_\xi$ in such a way that:

$$\begin{aligned}\mathcal{S}_\xi : &[\boldsymbol{q}_T(t)^\intercal, \boldsymbol{q}_L(t)^\intercal, \dot{\boldsymbol{q}}_T(t)^\intercal, \dot{\boldsymbol{q}}_L(t)^\intercal]^\intercal, \\ &\mapsto [\mathcal{T}(\boldsymbol{q}_T(t))^\intercal, \boldsymbol{q}_L(t)^\intercal, \dot{\boldsymbol{q}}_T(t)^\intercal, \dot{\boldsymbol{q}}_L(t)^\intercal]^\intercal\end{aligned} \tag{3}$$

where $\mathcal{T}$ is a linear transformation in $SE(2)$ that changes the torso's position q_x, q_y and heading direction q_{yaw}.

This is the most obvious but often ignored symmetry in a legged system, which applies to any gaits. It suggests a robot can start from anywhere in space with a certain height and move in any direction using the same gait without altering the leg movements. This is also referred to as the group of linear transformations in mechanics and they represent changes in coordinates without affecting the formula for differential equations of motion [10]. As for a planner system, it implies the model can also move in the opposite direction by changing $q_{\text{yaw}} = \pi$ rad in the inertial frame. This will be referred to as $\mathcal{S}_{\xi(\pi)}$ afterwords. However, it is important to distinguish this symmetry from the temporal symmetry mentioned in the previous definition. Even though in both cases, the robot is moving backward, the orientation q_{yaw} of the robot is not changed in the temporal symmetry.

3) Morphological Symmetry: In a similar fashion to the morphologies of animals in nature, most of the robots also possess a bilateral symmetry (left and right sides are mirrored images of each other with respect to the sagittal plane) that reduces complexity in design, manufacturing, and control. This symmetry will also introduce additional geometrical symmetries in gaits. The detailed discussion of modeling of articulated leg configurations has been omitted due to space constraints. In the following analysis, we assume that all legs have an identical structure and they are connected to the torso at the hip and shoulder joints such that the bilateral symmetry of the system with respect to the sagittal plane is retained (see the model in Fig1.B as an example).

Definition 6 (Morphological Symmetry): Assume a robot has the bilateral symmetry as described above, the permutations σ of the index set of four legs $L = \{\mathrm{LH}, \mathrm{LF}, \mathrm{RF}, \mathrm{RH}\}$ form a discrete symmetry subgroup G_σ. Morphological symmetry on the gait $\mathcal{O}$ is a function $\mathcal{S}_\sigma$:

$$\begin{aligned} \mathcal{S}_\sigma : &[\boldsymbol{q}_T(t)^\intercal, \boldsymbol{q}_L(t)^\intercal, \dot{\boldsymbol{q}}(t)_T^\intercal, \dot{\boldsymbol{q}}(t)_L^\intercal]^\intercal, \\ &\mapsto [\boldsymbol{q}_T(t)^\intercal, \sigma(\boldsymbol{q}_L(t))^\intercal, \dot{\boldsymbol{q}}_T(t)^\intercal, \sigma(\dot{\boldsymbol{q}}_L(t))^\intercal]^\intercal \end{aligned} \tag{4}$$

III. Results

This section showcases our primary discoveries and illustrates how different parameter bifurcations break symmetries in a simplistic model in distinct ways, leading to various quadrupedal gaits and footfall patterns. In particular, we employed numerical continuation techniques outlined in our earlier research [11] and sought out periodic solutions. In this study, we revealed four unique quadrupedal gaits (pronking, bounding, half-bounding, and galloping) that demonstrate interconnections through diverse parameter bifurcations. This system has been developed in MATLAB, and the source code is available for download from our GitHub repository [1]. Please also refer to the multimedia file or visit the web page [2] to view animations of the gaits in this study.

A. Pronking and Bounding Gaits

1) Pronking (PF)*:* is a quadrupedal gait frequently observed in quadrupedal animals, characterized by the synchronized movement of all four legs. During a single stride, there is only one flight phase followed by a stance phase, during which all four legs make contact with the ground, moving in precisely the same manner. This results in zero torque on the torso and the torso has no rotational motion throughout the stride ($\dot{q}_{\text{pitch}} = 0\ [rad/s]$). Our parameter continuation process initiated with a simple seed solution, where the model executed an in-place jump, with all four legs aligned vertically downward ($\dot{q}_x = 0\ [\sqrt{gl_o}]$ and $\dot{q}_{\text{pitch}} = 0\ [rad/s]$). When the overall energy in the system was modified, the resulting solutions constituted a one-dimensional curve (blue curve in Fig. 2) with varying average speeds. Multiple consecutive keyframes of the pronking gait, starting with an initial speed of $5.2\ [\sqrt{gl_o}]$, at the instances of the apex, touchdown, and liftoff, were illustrated in Figure 2(a). In our definitions, the pronking gait exhibits the largest number of symmetries. It is characterized by the Time-Reversal Symmetry $\mathcal{S}_\psi$, which means that by reversing the signs of the velocity states, one can immediately identify another periodic motion without changing the configurations or requiring additional numerical integration. As shown in Figure 2(a), this implies that examining the keyframes of the pronking gait in the sequence of 4-3-2-1 also represents a pronking gait moving in reverse with a negative horizontal speed. Furthermore, it is worth noting that due to the uniformity of the

[1] https://github.com/DLARlab/BreakingSymmetryLeadstoDiverseGaits
[2] https://dlarlab.syr.edu/research/breaking-symmetries/

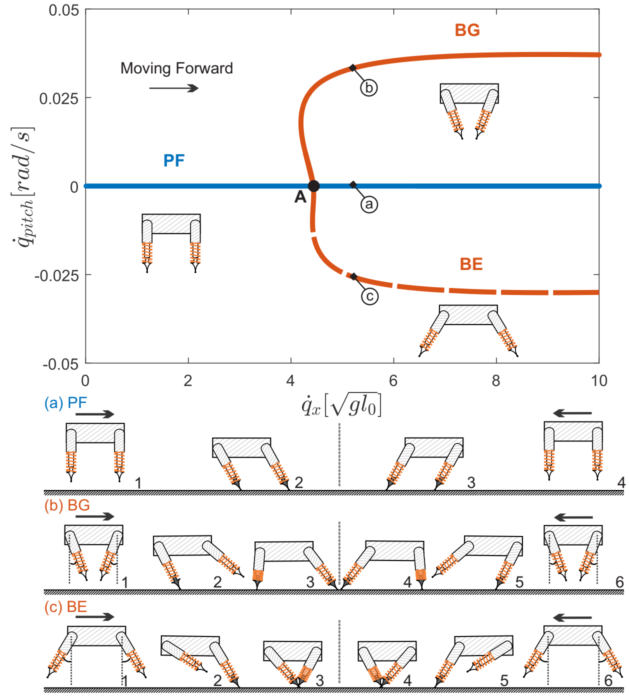

Fig. 2. Gait branches of pronking forward (PF), bounding with gathered suspension (BG), and bounding with extended suspension (BE) on the Poincare section with the torso's horizontal velocity $\dot{q}_x$ as the horizontal axis and pitching velocity $\dot{q}_{\text{pitch}}$ as the vertical axis. Examples of each gait (a-c) are shown as successive keyframes at the touch-down, lift-off moments, and the apex at the bottom. Black feet are used to highlight the legs in stance.

leg motions, the pronking gait preserves all morphological symmetry related to leg permutations $\mathcal{S}_\sigma$, where $\sigma \in \mathbb{S}_L$ ($\mathbb{S}_L$ denotes all permutations of the set L).

2) Bounding (BG and BE)*:* Compared to pronking gaits, bounding gaits exhibit a breakdown in the coordination between the front and hind legs. Despite the synchronized movements within the front and hind leg pairs, there is a phase delay between legs on the same sides, leading to two touchdown and liftoff events within a single stride. Our model yielded two distinct types of solutions that adhere to this pattern. In the first type of bounding gait, as depicted in Fig. 2(b), the hind leg pair makes initial contact with the ground, followed by the front legs, causing the leg pairs to converge inward during the flight phase. This particular gait is referred to as *bounding with gathered suspension*, as described in [7], and we'll abbreviate it as BG hereafter. In Fig. 2, these solutions are represented by the solid orange curve, which bifurcates from the PF branch at $\dot{q}_x = 4.4\ [\sqrt{gl_o}]$ (designated as black dot A). The other type of bounding gait is characterized by the opposite sequence of touch-downs, as shown in Fig. 2(c), where the front legs touch the ground first, followed by the hind legs. Consequently, the swing leg pairs extend outward during the flight phase, termed *bounding with extended suspension* (BE). In Fig. 2, these solutions are represented by red dashed curves, connected to the pronking branch at the same bifurcation point A. Although the footfall patterns and swing leg behaviors of these two bounding gaits differ, they share common underlying symmetries. Both BG and BE possess an equal number of morphological symmetries $\mathcal{S}_\sigma$, where $\sigma \in \{$(LF,RF), (LH,RH), (LF,RF)(LH,RH)$\}$. This means that the system states of legs within the front or hind leg pairs follow identical time series. Consequently, altering the states within one or both leg pairs will not impact the system's dynamics. Contrasting with the PF gait discussed in the previous section, the distinguishing feature in the bounding gaits lies in the symmetry breakdown between the front and back leg motions, represented by σ = (LH,LF)(RF,RH). This introduces a phase lag in the leg pairs, which can be either positive or negative, giving rise to two new gaits: BG and BE, originating from point A. Furthermore, it is noteworthy that new periodic orbits can be identified for both BG and BE gaits by merely reversing all the speeds while retaining the same system configurations. This highlights the presence of time-reversal symmetry ψ. Without performing an additional numerical search, the keyframes displayed in Fig. 2 (b)&(c) represent two distinct periodic solutions with opposite moving directions: one advances from the 1st frame to the 6th frame with a positive speed, while the other moves in the reverse direction, from the 6th frame back to the 1st frame with a negative speed.

B. Pronking and Bounding Gaits of an Asymmetric Model

The time-reversal symmetry ψ observed in the pronking and bounding gaits illustrated in Fig. 2 offers a practical method for identifying two periodic motions within a single numerical search. Nevertheless, as demonstrated in this subsection, the presence of this symmetry is strongly contingent on the morphological symmetry concerning the frontal plane, where the mechanical components of the system's anterior and posterior are mirrored. To be more precise, our findings indicate that when the COM is shifted away from the body's central point, the pronking and bounding gait branches discussed in the previous section undergo rapid changes.

We conducted numerical continuations using two models with distinct parameters, where $l_{b,H}$ was set at 0.4 $[l_o]$ for the model with the COM closer to the posterior, and 0.6 $[l_o]$ for the model with the COM closer to the anterior. To clearly differentiate the results, we utilize a trapezoidal shape to represent the robot's torso, positioning the COM closer to the side with the longer base. During forward motion ($\dot{q}_x > 0$), the pronking branch PF is no longer present in both models. This absence is attributed to the differing lever arm lengths of the four legs, preventing the leg forces from producing zero torque on the torso during the stance phases when all four legs were fully synchronized. In each of the models, we observe only one type of bounding gait at a given speed. In the model with $l_{b,H} = 0.4$ $[l_o]$ (as shown in Fig. 3(d)), BE appears within lower speed ranges (indicated by the dashed orange curve), while BG emerges (solid orange curve) as the exclusive gait at speeds exceeding $\dot{q}_x = 3.2$ $[\sqrt{gl_o}]$. Conversely, in the model with the reversed COM shift (depicted in Figure 3(e)), BE (represented by the dashed red line) is the sole bounding gait seen at speeds surpassing $\dot{q}_x = 2.5$ $[\sqrt{gl_o}]$. In comparison to the symmetrical model discussed in the previous section, both

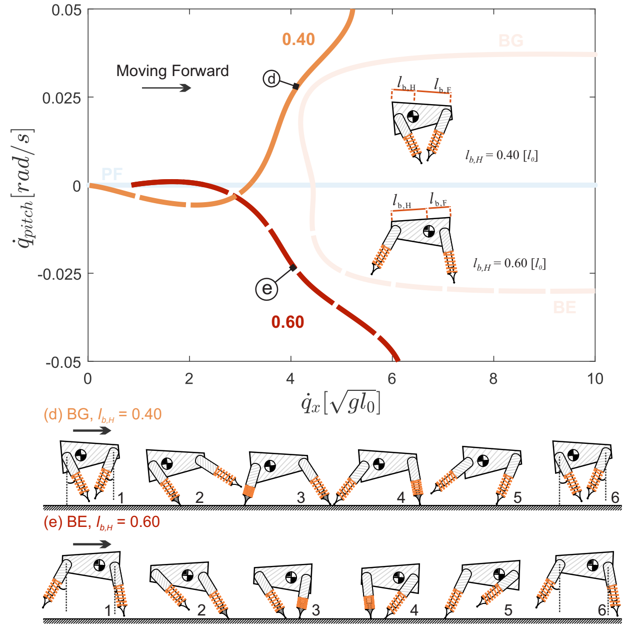

Fig. 3. The figure displays bounding gait branches for asymmetrical models where $l_{b,H} \neq 0$. Two specific cases, $l_{b,H} = 0.40$ $[l_o]$ and $l_{b,H} = 0.60$ $[l_o]$, are highlighted, with their corresponding solution branches illustrated in orange and red, respectively. Solid lines represent bounding gaits with gathered suspensions (BG), while dashed lines depict bounding gaits with extended suspensions (BE). In contrast to the bounding gaits of the symmetrical model shown in Fig. 2, our numerical analysis indicates that as the COM shifts closer to the rear, BG manifests at intermediate speeds (d). In contrast, when the COM is nearer to the front at $l_{b,H} = 0.60$ $[l_o]$, BE remains the exclusive bounding gait.

bounding gait branches are only present within intermediate speed ranges and vanish rapidly when the speed exceeds $\dot{q}_x = 5$ $[\sqrt{gl_o}]$. However, it is important to observe that, as depicted in Fig. 3(d)&(e), the pitch angles are no longer zero, and the magnitudes of leg angles differ during the apex transition in the first and last frames. This indicates that the time-reversal symmetry ψ is no longer preserved for a gait originating from a model with $l_{b,H} \neq 0.50$ $[l_o]$. Hence, reversing the speeds (via ψ) does not result in discovering gaits that moved backward *i.e.*, observing the frames in the sequence of 6-1 does not represent a periodic motion for the same model. Furthermore, for a given speed, the model with full symmetry illustrated in Fig. 2 has two feasible bounding gaits readily available. For the asymmetrical model depicted in Fig. 3, only one bounding gait exists, and the viable footfall pattern depends on the location of the COM.

IV. Conclusions

In this study, we conducted a comprehensive exploration of the symmetries in quadrupedal legged locomotion, employing the principles of group theory. These solutions were identified using a single energy-conserving model which represent distinct oscillation modes within the same hybrid system, triggered solely by initial conditions like forward speed and the torso's height. This work not only provides crucial insights into the rationale behind utilizing multiple gaits at varying speeds but also holds the promise of an efficient and versatile strategy for generating reference trajectories for robotic systems with desired footfall sequences.

REFERENCES

[1] M. Hildebrand, "Symmetrical gaits of horses," *Science*, vol. 150, no. 3697, pp. 701–708, Nov. 1965. [Online]. Available: https://doi.org/10.1126/science.150.3697.701

[2] ——, "The quadrupedal gaits of vertebrates," *BioScience*, vol. 39, no. 11, pp. 766–775, Dec. 1989. [Online]. Available: https://doi.org/10.2307/1311182

[3] M. H. Raibert, "Running with symmetry," *The International Journal of Robotics Research*, vol. 5, no. 4, pp. 3–19, Dec. 1986. [Online]. Available: https://doi.org/10.1177/027836498600500401

[4] H. Razavi, A. M. Bloch, C. Chevallereau, and J. W. Grizzle, "Symmetry in legged locomotion: a new method for designing stable periodic gaits," *Autonomous Robots*, vol. 41, pp. 1119–1142, 2017.

[5] D. Ordonez-Apraez, M. Martin, A. Agudo, and F. Moreno-Noguer, "On discrete symmetries of robotics systems: A group-theoretic and data-driven analysis," *arXiv preprint arXiv:2302.10433*, 2023.

[6] H. Razavi, A. M. Bloch, C. Chevallereau, and J. W. Grizzle, "Symmetry in legged locomotion: a new method for designing stable periodic gaits," *Autonomous Robots*, vol. 41, no. 5, pp. 1119–1142, July 2016. [Online]. Available: https://doi.org/10.1007/s10514-016-9593-x

[7] M. Hildebrand, "Analysis of asymmetrical gaits," *Journal of Mammalogy*, vol. 58, no. 2, pp. 131–156, May 1977.

[8] A. M. Pace and S. A. Burden, "Piecewise-differentiable trajectory outcomes in mechanical systems subject to unilateral constraints," in *Proceedings of the 20th International Conference on Hybrid Systems: Computation and Control*, 2017, pp. 243–252.

[9] J. S. Lamb and J. A. Roberts, "Time-reversal symmetry in dynamical systems: A survey," *Physica D: Nonlinear Phenomena*, vol. 112, no. 1-2, pp. 1–39, Jan. 1998. [Online]. Available: https://doi.org/10.1016/s0167-2789(97)00199-1

[10] S. F. Singer, *Symmetry in mechanics: A gentle, modern introduction*. Springer Science & Business Media, 2001.

[11] Z. Gan, Y. Yesilevskiy, P. Zaytsev, and C. D. Remy, "All common bipedal gaits emerge from a single passive model," *Journal of The Royal Society Interface*, vol. 15, no. 146, p. 20180455, Sept. 2018. [Online]. Available: https://doi.org/10.1098/rsif.2018.0455